6th Canadian Conf. Earthquake Engineering / Toronto / 1991 / 6ème Conf. Canadienne Sismique

The effect of floor-slabs on the behaviour of beam-column connections under seismic loads

S.J. Pantazopoulou[1] and A. Bas[2]

ABSTRACT

The experimental behaviour of a full-scale reinforced concrete beam-column subassembly with floor-slabs is presented. The specimen, tested at the University of Toronto, modeled an interior frame connection and was subjected to bi-directional cyclic loads simulating earthquake effects. Effective slab width, joint behaviour, transverse beam torsion / weak axis bending, and interaction between the two orthogonal directions are investigated. The essential features of the mechanism controlling the flow of connection forces into the joint are discussed in light of the experimentally obtained strain fields.

INTRODUCTION

Behaviour of beam column connections with floor-slabs has been the focus of many research studies since the early 1980's, after reports from the U.S.-Japan cooperative experimental program indicated that monolithic floor-slabs may cause dramatic overstrength to the supporting beams in frame structures subjected to lateral loads (Durrani and Wight 1982; Otani et al. 1984). However, beam flexural overstrength if not accounted for in the design phase may be undesirable because it may increase the shear demand on the joint or defeat the weak-beam / strong-column philosophy of connection design (Paulay et al. 1978). Experimental studies conducted during the past decade (Zerbe and Durrani 1985 and 1988; French and Boroojerdi 1989; Kurose et al. 1988; Pantazopoulou and Qi 1990; Bas 1990) have helped to identify the cause of the so-called "slab contribution" effect which is now attributed to the kinematic constraints that exist between monolithically cast floor-slabs and their supporting beams along the interface of the two elements (Pantazopoulou et al. 1988). During earthquake action, lateral loads induce a linear moment variation along the beam spans, the moments reaching a maximum value at the faces of the columns within each bay. If the moments are negative (hogging), the upper beam fibres are in tension, and because of the limited tensile resistance of concrete, the neutral axis is well below the slab thickness. The deformation of the longitudinal beam fibres is approximately proportional to the distance from the neutral axis of the beam. Because of the kinematic constraints mentioned above, longitudinal deformations in the slab are identical to those of the beam along the common boundary of the two elements. However, the beam elongation is felt to a lesser extent at large transverse distances from the main beam, and this decay is manifested by a shear-lag effect in the slab diaphragm. Longitudinal elongations in the slab require that the slab reinforcement be in tension; the total force acting over the distance from the neutral axis generates an additional moment resistance which, when detected in experiments, is termed "slab contribution".

Because of the brittle tensile behaviour of concrete, surface elongations (caused by hogging moments) become more dramatic after cracking, and are more pronounced at higher levels of lateral displacements. For this reason, slab membrane actions increase with the extent of cracking and therefore with increasing lateral storey displacement (or lateral drift).

The initial results described above, were naturally followed by an array of unanswered questions (Ammerman and French 1989; Bas 1990). For example, the role of transverse beams in the mechanics

[1]Assistant Professor, Dept. of Civil Engrg., University of Toronto, M5S-1A4, CANADA
[2]M.A.Sc., Billur Sok. 70/4, K.Esat, Ankara, Turkey 06700

of the connection is not yet clearly understood. The mechanism by which forces are transferred from the slab to the joint must be explained; there is a need to establish whether joint shear demand increases as a result of slab participation, and, if so, to determine the degree of improvement of joint resistance which is also likely to result from the confining action of the slab. A rigorous explanation is necessary for the conflicting experimental and theoretical evidence of slab-beam behaviour under positive (sagging) moments, particularly in cases of interior slab-beam-column connections where the slab is nominally in tension on one face of the column, and in compression on the other. It is imperative that such an explanation be unbiased from the particular details of the simplified specimen tested in the laboratories; certain pronounced features of the response that have been observed in laboratory tests of single connection specimens are believed to be directly related to the details of the load setup and are not representative of the behaviour of connections in actual continuous structures.

This paper documents results of a single connection test carried out at the University of Toronto (Bas 1990). The specimen was a full-scale, statically determinate assembly of an interior slab-beam-column connection. Loading was applied along the two principal directions of the specimen geometry, simulating bi-directional earthquake effects. The aim of the paper is to provide experimental information as to such aspects of the behaviour that relate to the physical arguments outlined in the preceding.

EXPERIMENTAL PROGRAM

Specimen Geometry

The specimen represents an interior connection of a typical reinforced concrete multi-storey frame structure with the plan view shown in Fig. 1. The scale, geometry and load setup of the structure are similar to those of the larger number of specimen tested recently by other investigators, so as to enhance the available data base. The beam ends of the specimen are assumed to correspond to the approximate location of the inflection points at the midspans of the complete frame structure, and are loaded so that the force-boundary conditions of zero flexural moment are approximately satisfied. Although this convention is common amongst all single connection specimen that have been tested thus far, it must be emphasized that the remaining (displacement and shear) boundary conditions are insufficiently modeled at the edges of the specimen; this generally leads to concentrated load effects which must be taken into consideration in interpreting the results.

Specimen dimensions are illustrated in Fig. 2. Column ends were supported by spherical hinges; because of the physical dimensions of the hinges, the actual inflection points were somewhat shifted during the test outside the column height. (The resulting effective height of the column was 3.0 m which led to a relatively low level of shear stress in the column.)

Beam cross-sections were 380 mm high by 220 mm wide in both directions. The columns had a 400 mm square cross-section. Slab was 100 mm thick. Beam ends were extended beyond the slab edge (Fig. 2) to provide a loading region which would support the load actuators during the test, and to minimize the concentrated load effects which are induced to the slab by the loading system. To reduce the likelyhood of a localized failure, beam cross-sections were wider at these locations with dimensions of 380 mm by 320 mm. All four beams were reinforced with 4-#15 (15 mm diameter) top, and 3-#15 bottom bars (corresponding reinforcement percentages computed over the gross-area were 0.96% and 0.71%). Beams were confined by #10 (10 mm) hoops placed at 90 mm spacing on centres (o.c.) along their entire length. The slab was reinforced at top and bottom with 8 mm bars placed at 200 mm spacing o.c. in the longitudinal and transverse directions. Slab and beam longitudinal bars running in the North-South direction were placed between the respective longitudinal bars in the East-West direction since the two groups of reinforcement crossed each other, and consequently the flexural strength of the beams in the North-South direction was slightly lower than that of the beams in the East-West direction.

The connection was designed with the aim to minimize the possibility of yielding in the column under simultaneous development of the beam strengths in the two orthogonal directions. As a result, columns were heavily reinforced with 12-#25 bars (ρ= 3.75%) and were confined by 4-leg #10 hoops placed at a 90 mm spacing o.c. The transverse reinforcement used for column confinement was extended along the height of the beam-column joint. Joint shear stress under unidirectional loads (estimated assuming that all beam bars and two slab bars at each face of the beam had yielded, and that actual steel properties would be enhanced by 25% due to strain hardening) was 0.83 $\sqrt{f'_c}$ (MPa) which satisfies the limits established by the CSA (1984) Code. The ACI-ASCE 352 Recommendations (1985) were also satisfied in the joint design except for the limitation of the maximum column bar diameter passing through the joint.

To avoid localized shear failure at the loading points (beam ends), in addition to the hoops, #10 bent bars were placed as additional shear reinforcement. Because of the limited space in the laboratory, the anchorage length requirements at the beam ends were not satisfied and for this reason beam bars were welded to 1 in steel plates.

Average compressive strength of the concrete measured at the time of the test was 44.5 MPa. Yielding stresses of the reinforcement were 607 MPa, 454 MPa, 484 MPa, and 506 MPa for #8, #10, #15 and #25 bars respectively. The corresponding ultimate stresses were 685 MPa, 640 MPa, 646 MPa, and 687 MPa. Load and displacement records, and strain measurements were obtained at critical locations in all the components of the specimen. In addition, surface strains of the concrete were obtained using Zurich gauges at several stages during the test.

Test Setup and Loading Programme

In the beginning of the test, the column was loaded axially at the top by a 700 kN force (approximately 20% of the column balanced axial load, P_b) which was held constant throughout the test. This load was applied to simulate the self weight of the superstructure in real buildings, and also to confine the spherical bearings against possible lateral slippage due to shear.

Cyclic loads were applied on the beam ends, introducing moment transfer at the connection similar to that occurring under seismic attack. The loading program was carried out under displacement control, with the associated storey drift being the controlling parameter of the loading history. Displacement levels corresponding to 0.5%, 1.0%, 1.5%, 2.0% and 3% drift were subsequently applied to the specimen.

At each drift level, the pattern of the cyclic load history adopted was as shown in Fig. 3. The stronger beam (E-W direction) was the main direction of the test. During the first stage at each displacement level, only the E-W direction was loaded, introducing uni-directional loading to the connection. At the second stage, both directions were loaded simultaneously, modeling bi-directional earthquake loads occurring at a 45 degree angle with the E-W direction. At the end of the planned displacement history, the E-W direction was subjected to an additional cycle up to the limiting stroke of the actuators.

EVALUATION OF THE TEST RESULTS

In the following discussion, positive displacement or load is defined as upwards, and positive rotations or moments are associated with positive displacements and loads respectively. Tensile strains are considered positive for both steel and concrete.

Discussion of the Overall Response

The load-displacement histories of the East and South (strong and weak) beams of the specimen are given in Fig. 4. First yielding occurred in the strong beams at 1% storey drift under positive load, at which point the load-displacement response curve is characterized by a marked change of apparent stiffness. In contrast, for negative bending, there is a gradual increase of load with displacement without abrupt stiffness change up to 3% storey drift. The relative magnitudes of the loads in the positive and the negative bending cases were at a ratio of 1:2 for the stronger beams (East and West), and approximately 1:2.5 - 1:3 for the weaker beams (North and South). Due to uneven yielding under positive and negative bending, displacement ductilities in the former case were several times those observed in the latter case, although the overall displacements applied in the two directions were the same.

The ultimate flexural capacity of the strong beams reached 155 kN-m and 304 kN-m under positive and negative bending respectively. It is noteworthy that the corresponding estimates of beam flexural resistances using actual material properties were 106 kN-m and 135 kN-m, computed by ignoring the slab contribution. The discrepancy of values in the case of negative bending highlights the dramatic influence of the slab reinforcement in enhancing the negative flexural resistance of the supporting beam, and the significant increase of joint shear as compared with the estimate that results from the ACI-ASCE 352 (1985) model.

Storey Shear Orbits

Although all beams maintained their strength throughout the test, in consecutive load cycles at a fixed displacement level, strength and stiffness degradation was observed and was more pronounced for negative bending (slab in tension) than for positive bending (slab in compression). Resistance reduction was manifested in the storey shear orbits shown in Fig. 5, along the two orthogonal directions of specimen geometry throughout the test. It was seen that during the bi-directional load cycles (2-nd and 3-rd load cycles at a given displacement level), a sharp decrease in resistance occurred in the direction of constant displacement, while load in the orthogonal direction was increased. The reduction exceeded 25% of the maximum load at any given cycle, and highlights the extent of interaction that exists between orthogonal directions in the connection. The reason why interaction is more pronounced under negative bending can be understood by reviewing the requirements of equilibrium of the slab panel; consider a quadrant of the specimen (including the slab), with the main beam subjected to a negative vertical displacement, while the transverse beam is restrained at its end against vertical movement. Due to the shear-lag effect, tensile stresses develop in the longitudinal slab reinforcement along the face of the connection between the slab and the transverse beam. Because of these stresses, equilibrium of moments in the slab about any vertical axis dictates development of tensile stresses in the transverse slab reinforcement along the face of the connection between the slab and the main beam. Therefore, under unidirectional loads, the entire slab reinforcement is placed under tension. Addition of loads in the orthogonal direction (bi-directional load case), produces the same pattern of stresses on the reinforcement. Equilibrium in the first direction at a given displacement level can be now attained at a lower level of externally applied load; the resulting load difference is detected as strength reduction in the storey shear orbits.

Transverse Beams

Torsional cracking was observed in the North and South beams while unidirectional loads were applied in the East West direction at 1.5% storey drift. The cracks were located near the column, and were at right angles in the opposite sides of the beam. The cracks on the side of the transverse beam facing the slab-in-compression quadrant were about twice as wide as those measured on the other side (facing the slab-in-tension quadrant).

Other than torsional cracks, some vertical cracks at the side of the transverse beam, where the main beam was under positive bending, were observed at high deformation levels (3% storey drift). This, together with the existence of wider torsional cracks on that side illustrates that the amount of weak axis bending was significant in the transverse beam. Torsional deformations were observed to increase under bi-directional loading, when transverse beams also carried out-of-plane flexural loading. This is likely to be an indication of stiffness reduction resulting from the interaction of weak and strong axis moments with torsion along the beam.

Behaviour of the Slab

Slab participation was evident from the crack patterns observed on the top and bottom faces of the slab, and from extensive strain measurements obtained either by strain gauges attached on the reinforcement or from Zurich targets attached on the surfaces of the concrete. The surface cracks depicted in Fig. 6 are characterized by two separate patterns which became interwoven as the level of lateral drift increased. The first pattern consists of extensive cracks parallel to the faces of the column; these cracks formed around the connection and spread transversely into the slab, in directions perpendicular to that of the applied load. The second pattern consists of inclined cracks fanning at 45° near the beam ends; these cracks were initiated around the loading points and spread with increasing level of load towards the middle of the beam length. They also extended at 45° downwards in the beam web and are believed to be an indication of concentrated load effects associated with the experimental setup used to enforce the condition of zero moment at the beam ends. (The second crack pattern described is not representative of the general behaviour of connections with floor slabs in indeterminate structures.)

Strains recorded in the slab reinforcement were tensile regardless the direction of loading, except for the top slab reinforcement adjacent to the column, which experienced compressive strains under positive bending and up to 1.5% storey drift. Figures 7(a)-(b) plot the strain distribution of top and bottom slab bars at the East face of the column under negative and positive bending respectively. Longitudinal slab strains recorded at the face of the transverse beam were typically higher near the column, decreasing with transverse distance from the support in the case of negative bending. This result concurs with the proposition of "shear-lag" in the slab diaphragm, and illustrates the degree of approximation implicit in the traditional assumption of plane-sections which is commonly used in analyzing monolithic R.C. tee-beams.

The mechanism of slab participation is better illustrated in the measured surface strains of concrete; these strains are averaged over a square grid of targets spaced at 20 cm and therefore are less sensitive to local slip disturbances than the reinforcement measurements. Table 1 summarizes the principal strains recorded during the first uni-directional excursion to 2% drift. Whereas the slab in tension side is under net elongation in both principal directions, in contrast, a diagonal compression field characterizes the slab in compression case, particularly around the column (at some distance from the area of influence of the concentrated loads which act at the beam ends). It is noteworthy that longitudinal steel strains at the same locations were tensile (Fig. 7(b)), suggesting than an amount of relative slip occurred between concrete and slab reinforcement.

To quantify the contribution of slab to the beam flexural resistance from the experimental results, beam properties were computed analytically assuming various effective slabs widths, equal to multiples of the beam depth, d. These computed moment-curvature relationships were compared with the experimentally obtained moment-curvature envelopes for the strong beam. From this comparison, it was found that for negative bending, at 2% lateral drift, the effective slab was 1.5 times the beam depth (measured on each side of the beam web); however, this quantity increased to 2-2.5 times the beam depth for 3% and 6% storey drift respectively. Under positive bending, the effective slab remained almost constant throughout the test, (approximately twice the beam depth on each side of the beam web); it is believed that the insensitivity of the computed moment-curvature relations to further increases in the assumed effective widths is probably a consequence of the limited amount of tension reinforcement at the bottom of the beam when the slab is in compression.

Joint Performance

Figure 8 plots hoop strains recorded in joint hoops in the E-W direction. Evidently, bottom hoops were overstressed when compared to the top ones; this indicates superior shear resistance at the upper part of the joint, likely to have resulted from the confining action of the floor-slabs. The total shear force introduced to the joint is estimated by considering equilibrium of forces in the column. (Column moments occurring at the top and bottom faces of the beam are computed from equilibrium of the entire specimen; joint shear is the slope of the column moment diagram within the beam depth.) Horizontal shear introduced to the joint directly by forces acting on the beam web was estimated using the actual yielding stress of the beam reinforcement. The resulting joint shear was 69%, 62% and 56% of the total joint shear measured under unidirectional loads at 2%, 3%, and 6% storey drifts respectively. This illustrates the increasing participation of other connection components (slab and transverse beams) in indirect loading of the joint, an effect that is not accounted for in the current design philosophy for joints.

CONCLUSIONS

Participation of slabs to the response of frame connections was investigated in light of experimental data obtained at the University of Toronto. Under uni-directional loads an effective width of slab approximately equal to 1.5-2 beam depths measured on each side of the beam web contributed to the flexural resistance of the supporting beams. However, a significant amount of interaction was detected between orthogonally placed beams when loads acted at a 45° angle relative to the principal directions of the connection geometry. The interaction was result of combined slab participation in the two orthogonal bending axes, but was also an indication of reduced joint shear resistance under bi-directional loads. Concrete strain records on the surfaces of the slab, in addition to reinforcement strain readings were considered in examining the mechanism of force transfer in the connection.

ACKNOWLEDGEMENTS

The experimental work presented in this paper was carried out at the University of Toronto, Canada. Financial support for the study was provided by NSERC grant No. OGP0042033.

REFERENCES

ACI Committee 318, Building Code Requirements for Reinforced Concrete, (ACI 318-83), American Concrete Institute, Detroit 1983.

ACI-ASCE Committee 352. 1985. Recommendations for Design of Beam-Column Joints in Monolithic Reinforced Concrete Structures. ACI Journal, Vol. 82(3), 266-283.

Ammerman, O. V., and French, C. W. 1989. R/C Beam-Column-Slab Subassemblages Subjected to Lateral Loads. J. Struct. Eng., ASCE, 115(6), 1289-1308.

Bas, A. 1990. Behaviour of Reinforced Concrete Beam-Column Connections With Floor Slabs Under Bi-directional Loads. Thesis submitted in conformity with the requirements for the degree of Masters of Applied Science in the Department of Civil Eng. of the Univ. of Toronto.

CSA Standard. 1984. Design of Concrete Structures for Buildings. CAN3-A23.3-M84, Canadian Standards Association, Rexdale, Ontario.

Durrani, A.J. and Wight, J.K. 1982. Experimental and Analytical Study of Internal Beam to Column Connections Subjected to Reversed Cyclic Loading. Report No. UMEE 82R3, Department of Civil Engineering, University of Michigan, Ann Arbor.

French, C. W. and Boroojerdi, A. 1989. Contribution of R.C. Floor Slabs in Resisting Lateral Loads. J. Struct. Eng., ASCE, 115(1), 1-18.

Kurose, Y., Guimaraes, G. N., Liu, Z., Krieger, M. E., and Jirsa, J. O. 1988. Study of R.C. Beam-Column Joints Under Uniaxial and Biaxial Loading. Report No. PMFSEL 88-2, Department of Civil Engineering, University of Texas at Austin, Austin, Texas.

Otani, S., Kabeyasawa, T., Shiohara, H., and Aoyama, H. 1984. Analysis of the Full-Scale Seven-Story Reinforced Concrete Test Structure. Earthquake Effects on Reinforced Concrete Structures, U.S.-Japan Research, ACI SP-84, American Concrete Institute, Detroit.

Pantazopoulou, S. J., Moehle, J. P., and Shahrooz, B. M. 1988. Simple Model for the Effect of Slabs on Beam Strength. J. of Struct. Eng., ASCE, 114(7), 2000-2016.

Pantazopoulou, S. J., and Qi, X. 1990. Proceedings of the 4-th U.S. National Conf. on Earthquake Eng., EERI, V. 2, 137-146, Palm Springs.

Paulay, T., Park, R., and Priestley, M. J. N. 1978. Reinforced Concrete Beam-Column Joints Under Seismic Actions. ACI Journal, 75(11), 583-593.

Zerbe, H. E., and Durrani, A. J. 1985. Effect of a Slab on the Behavior of Exterior Beam to Column Connections. Report No. 30, Department of Civil Eng., Rice University, Houston, Texas.

Zerbe, H. E., and Durrani, A. J. 1988. Seismic Behavior of Indeterminate R.C. Beam to Column Connection Subassemblies. Proceedings, 9-th World Conf. on Earthquake Eng., Tokyo, Japan.

TABLE 1
Principal Strains of the Slab - Unidirectional Loads at 2% Drift

Distance from column CL (mm)	Slab in tension			Slab in compression		
	ε1	ε2	θ (degrees)	ε1	ε2	θ (degrees)
1500	0.0025	0.00043	115.90936	8E-05	0.0011	51.623497
1300	0.0022	0.00015	115.04993	1E-05	0.0009	44.919891
1100	0.0019	0.00025	108.34632	-1E-05	0.0009	47.154427
900	0.0022	0.00056	86.115557	-4E-05	0.0008	57.353075
700	0.0028	0.00058	89.209529	-0.00023	0.001	63.541019
500	0.0035	0.00085	105.65342	-0.00061	0.0014	61.535667
400	0.0057	0.0008	112.52891	-0.00132	0.0022	59.415723

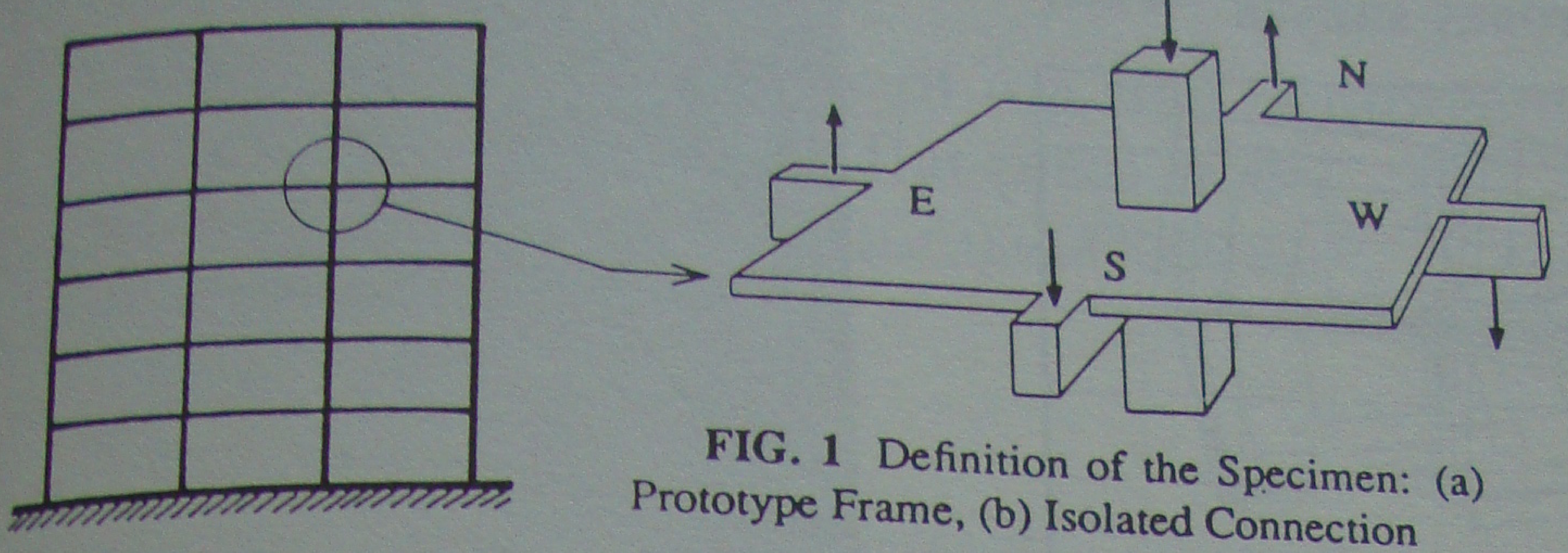

FIG. 1 Definition of the Specimen: (a) Prototype Frame, (b) Isolated Connection

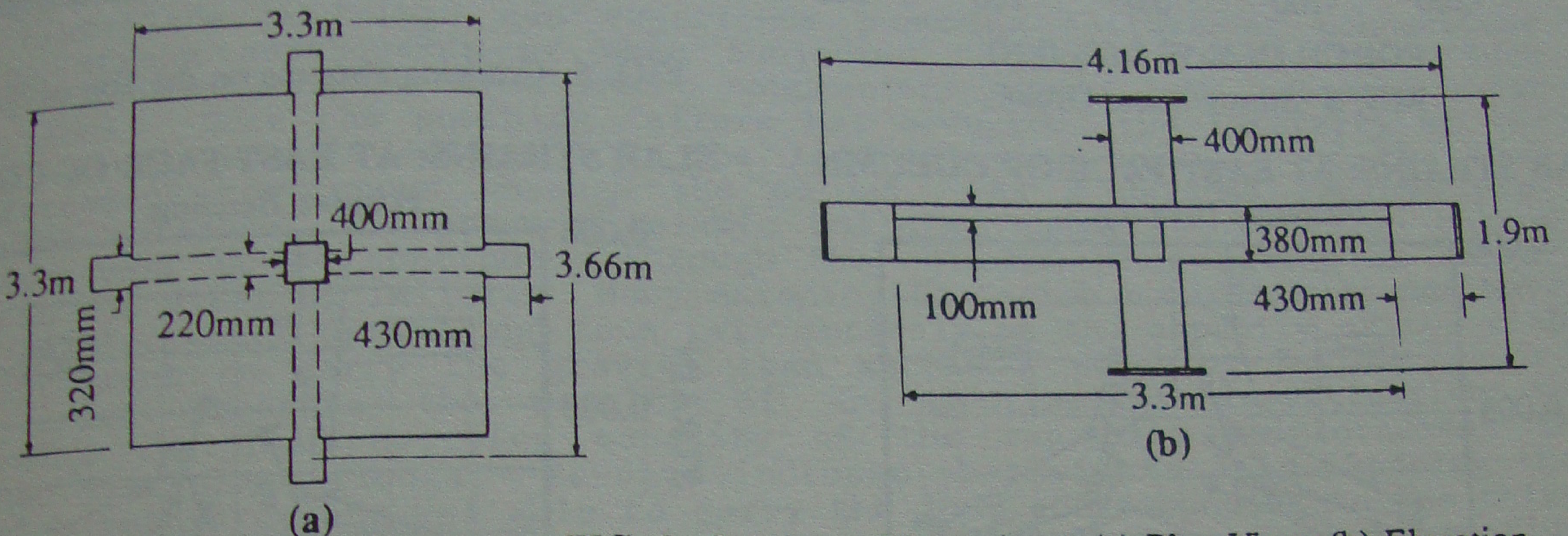

FIG. 2 Specimen Dimensions: (a) Plan View, (b) Elevation

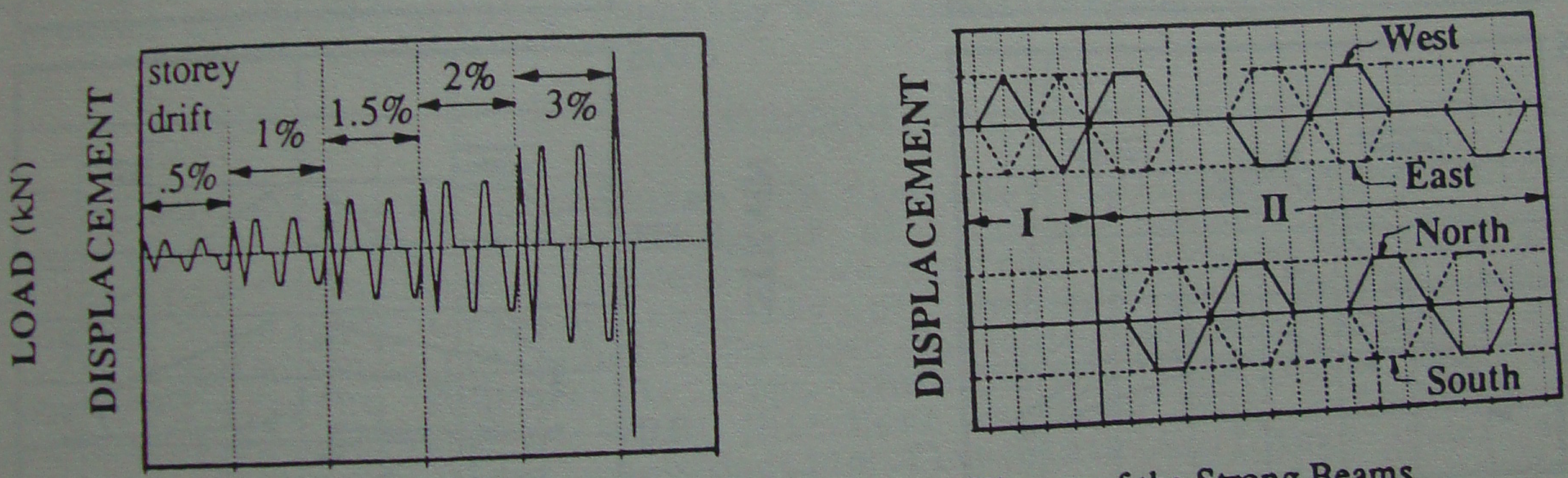

FIG. 3 Cyclic Load History: (a) Displacement History of the Strong Beams, (b) History of All Beams at Each Displacement Level

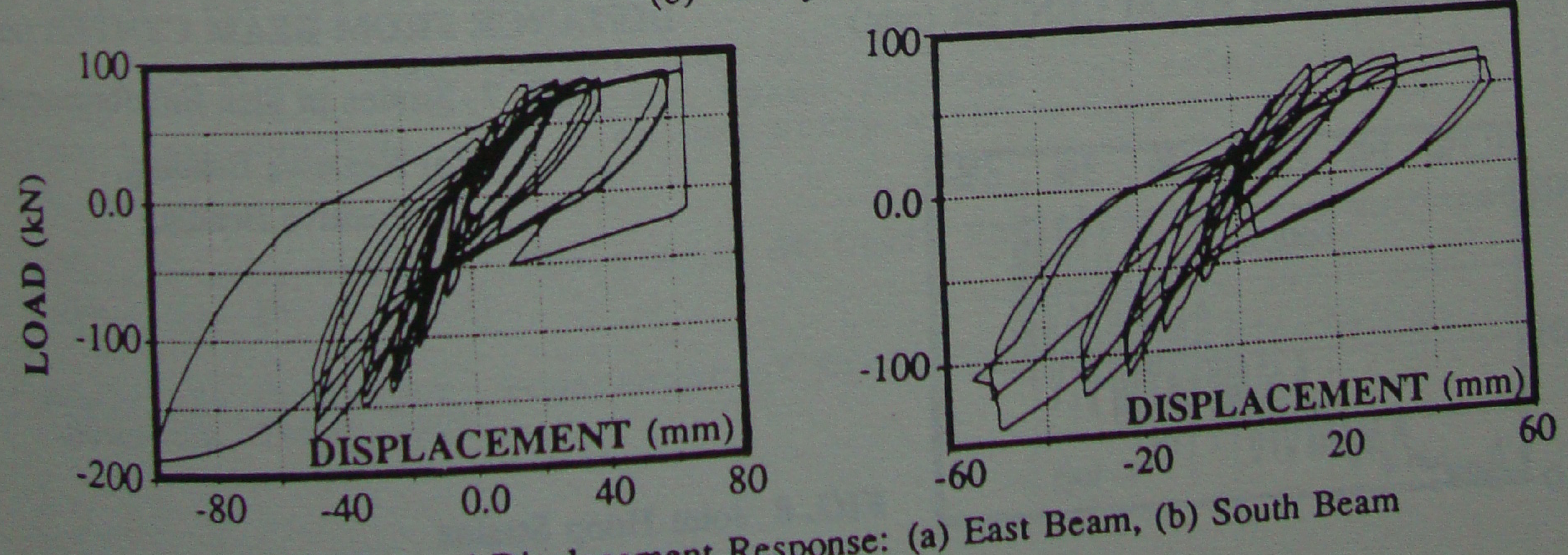

FIG. 4 Load-Displacement Response: (a) East Beam, (b) South Beam

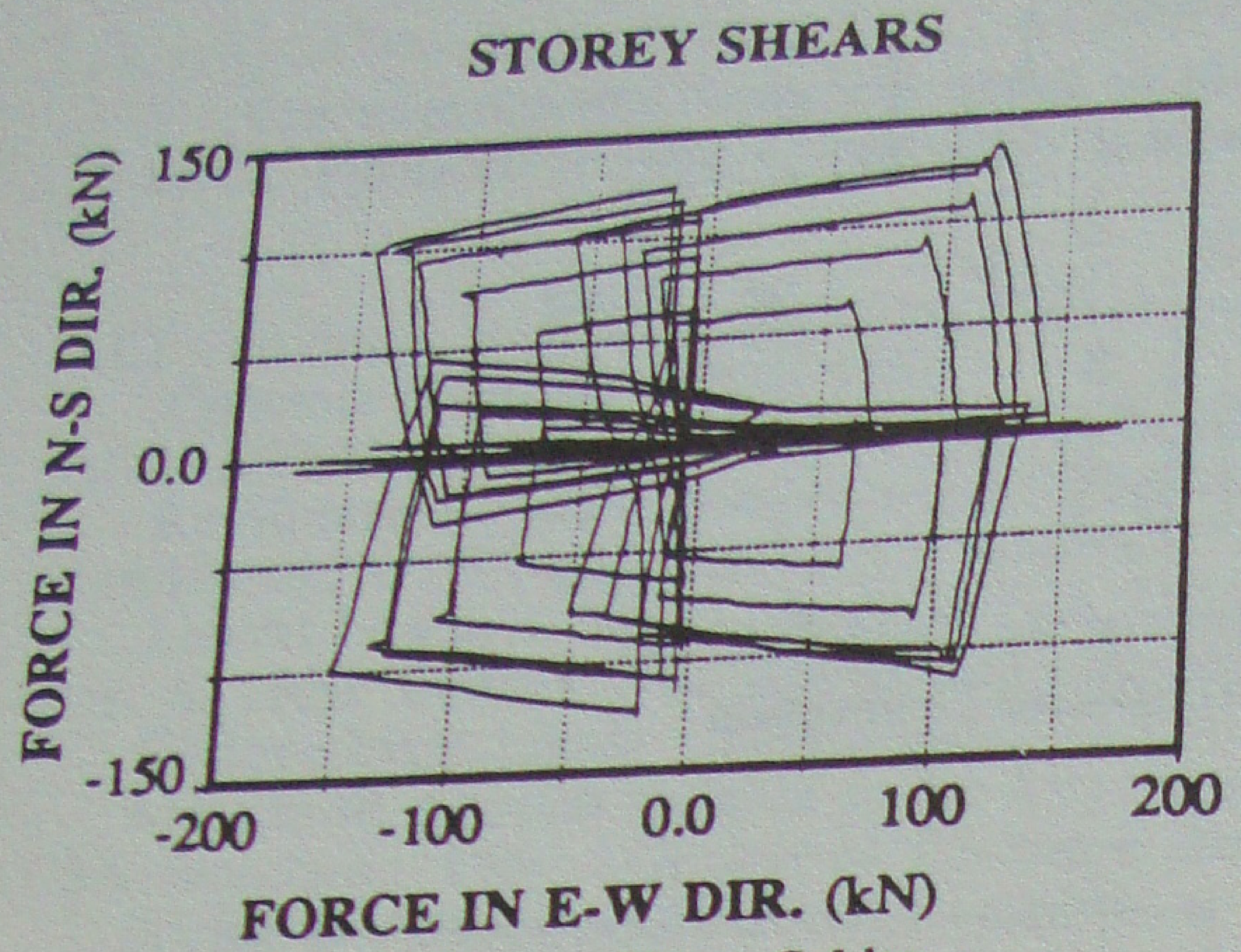

FIG. 5 Storey Shear Orbits

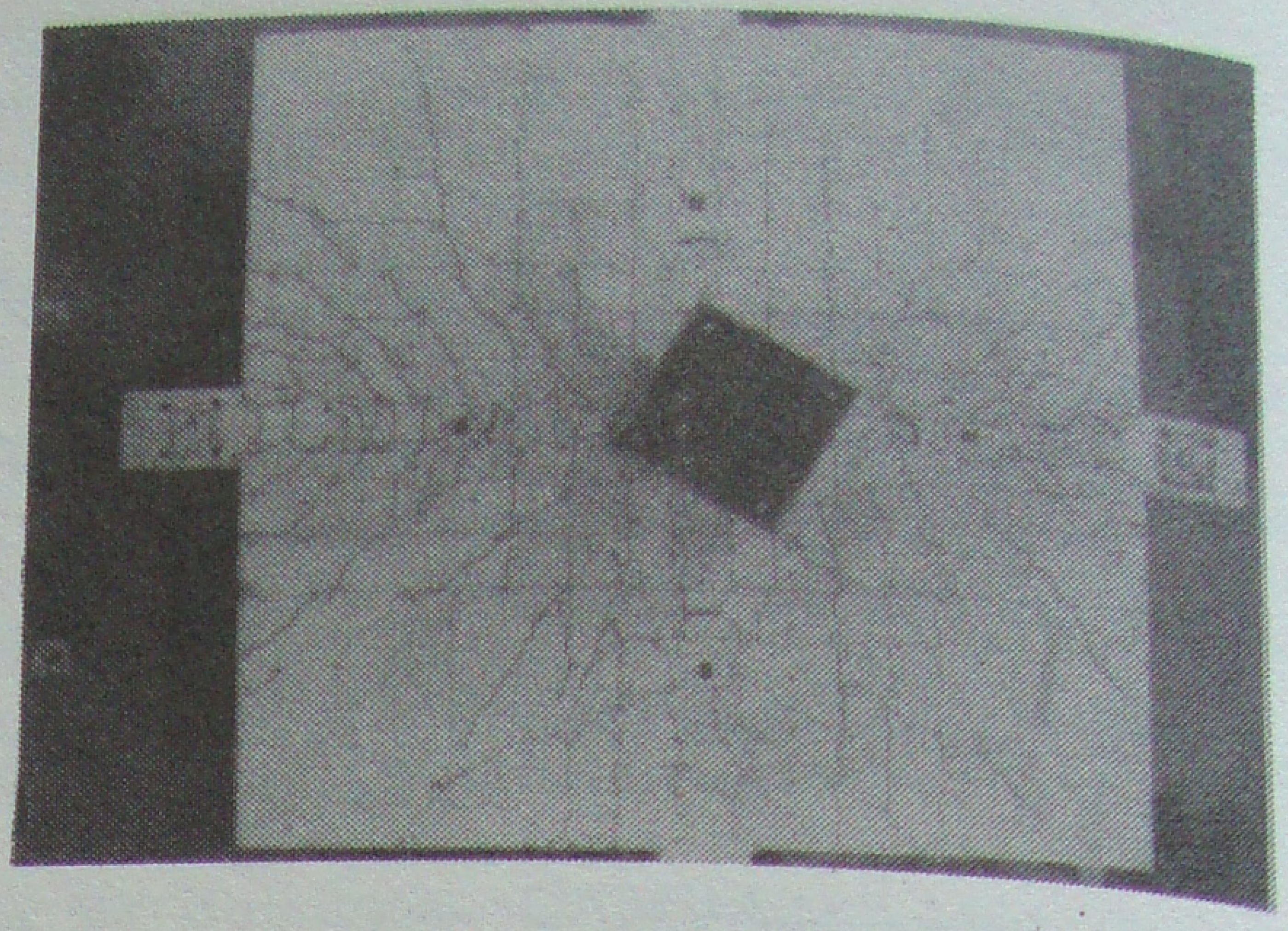
FIG. 6 Cracking Patterns on the Top of Slab

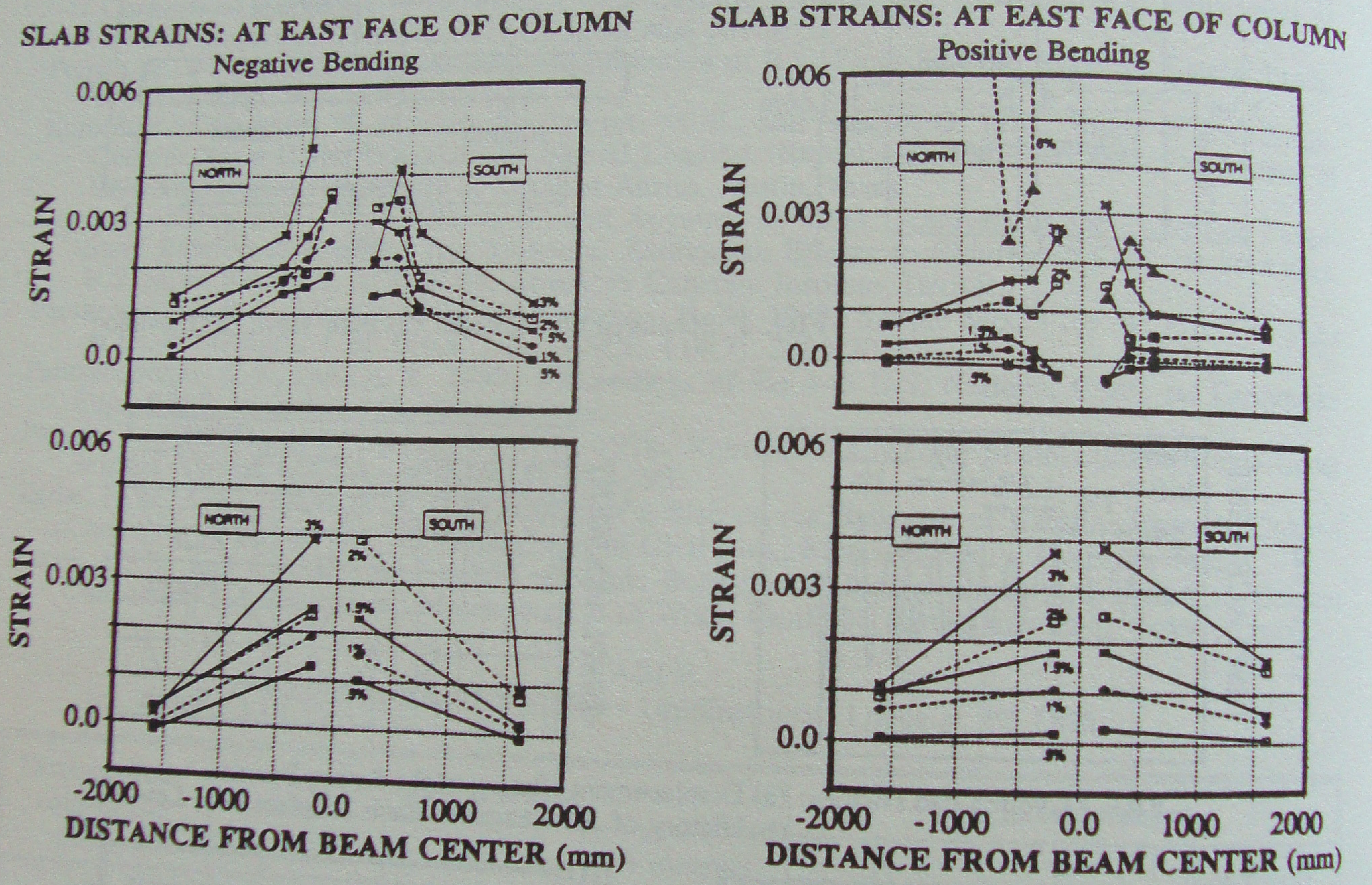

FIG. 7 Strains in Slab Reinforcement:

(a) Negative Bending,

(b) Positive Bending

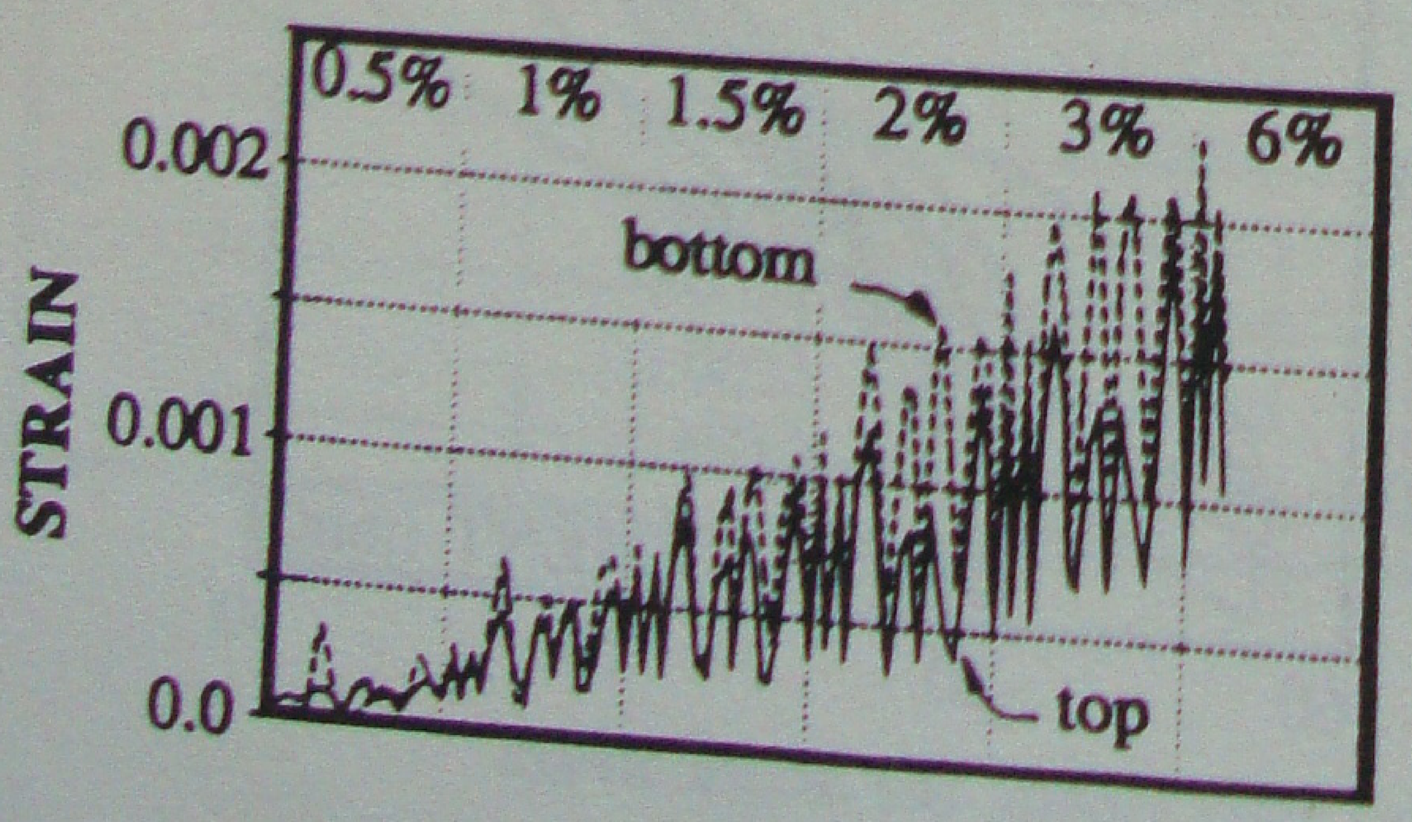

FIG. 8 Joint Hoop Strains